Topological Design of Pentamode Metamaterials with Additive Manufacturing

Shuhao Wu[b, a], Zhen Luo[a, *], Zuyu Li[a], Shutian Liu [b], Laichang Zhang [c]

[a] *School of Mechanical and Mechatronic Engineering*
University of Technology Sydney, Ultimo, NSW 2007, Australia
[*]***Corresponding author:*** *Phone: +61 2 9514 2994; E-mail: zhen.luo@uts.edu.au (Dr Z. Luo)*

[b] *State Key Laboratory of Structural Analysis for Industrial Equipment*
Dalian University of Technology, Dalian 116023, China.

[c] *School of Engineering*
Edith Cowan University, Perth, WA 6027, Australia

Abstract

Pentamode metamaterials (PMMs) are a new class of three-dimensional (3D) mechanical metamaterials, engineered to have unusual elastic property of vanishing shear modulus. Here 'penta' denotes five, referring to only one non-zero but five vanishing eigenvalues in the elasticity tensor of isotropic materials. PMMs gain their properties from their rationally designed structural architecture rather than their composition, mimicking the behaviour of fluids but are solid, hard to compress yet easy to deform. Compared to most up-to-date design methods based on rigid-body double-cone concept, this paper is to propose, for the first time, a new generative design method using topology optimization to find novel micro-lattice architectures, to enable pentamode properties through the overall elastic deformation of the micro-lattice. The design problem is then formulated to make the micro-lattice have a large but realistically attainable ratio of effective bulk modulus compared to the shear modulus, corresponding to the isotropic microstructure with the effective Poisson's ratio close to 0.5. The larger of the ratio, the better of the PMM solids to simulate liquids. Several numerical cases with the additive manufacture technique (SLM: selective laser melting) are used to demonstrate the effectiveness of the proposed topological design method in this paper.

Keywords: Topology optimization; Pentamode mechanical metamaterials; Three-dimensional solid microstructures; Additive Manufacturing.

1. Introduction

Metamaterials belong to new paradigmatic materials, artificially architected to have amazing effective properties of elasticity inaccessible in most conventional materials [1-4]. Here "meta" stands for materials with properties beyond natural ones. Metamaterials open a whole new chapter for creating new composite materials in association with unusual mechanical properties, and have sparked a surge of interests due to unlimited potential in triggering a myriad of applications, as diverse as bandgaps [5, 6], cloaking devices [7-9], electromagnetics [10], and transformation elastodynamics [11]. The composites consist of arrays of multiple individual lattice fashioned from conventional base materials, such as metals or plastics, but the materials are usually configured in periodic rather than random patterns. Hence, the metamaterials gain their unusual properties from their rationally designed geometrical shapes, not from their material chemical composition [12-17]. The research domain of metamaterials normally includes acoustic metamaterials with negative bulk modulus and/or mass density [18, 19], auxetics with negative Poisson's ratio (NPR) [20-22], materials with negative permeability [23, 24], materials with negative thermal expansion coefficient [25], cosserat and micropolar metamaterials [26], as well as the recently emerged PMMs transforming thermodynamics that are the major focus of this paper.

After 17 years of the first appearance in design [27], PMMs were manufactured in 2012 using the direct-laser-writing (DLW) optical lithography technique. The pentamode properties was achieved through the highly localized deformation by the fused point-like tinny tips of the rigid-body double-cones (Fig. 1) [28]. PMMs are composites of microstructures containing a sufficiently rigid isotropic phase and a sufficiently compliant isotropic phase, in which 5 out of 6 components (eigenvalues) of a diagonalised elasticity tensor are close to 0 [27]. In design, PMMs use one isotropic material with extremely large elastic moduli and another with extremely small elastic moduli, to build composites with effective elasticity tensors, to implement 3D transformation elastodynamics analogous to transformation optics in electromagnetic metamaterials. A perfect isotropic pentamode material has zero shear modulus and therefore a Poisson's ratio 0.5. As noted in the work [29-32], the liquids behaviour of pentamode materials can also be approximated by rationally designed 3D solid microstructures, which will not 'flow away' like conceptually perfect homogeneous pentamode materials. The microstructures can be designed to have a much larger bulk modulus (B) compared to its shear modulus (G). This unique property opens new possibilities. For instance, three-dimensional transformation acoustics

ideas [33, 34], for example, inaudibility cloaks, phononic bandgaps, acoustic prisms or new loudspeaker concepts, could become reality. We can tune local elastic wave propagation and control transformation elastodynamics architectures for acoustic 'unfeelability' cloaks invisible to sound.

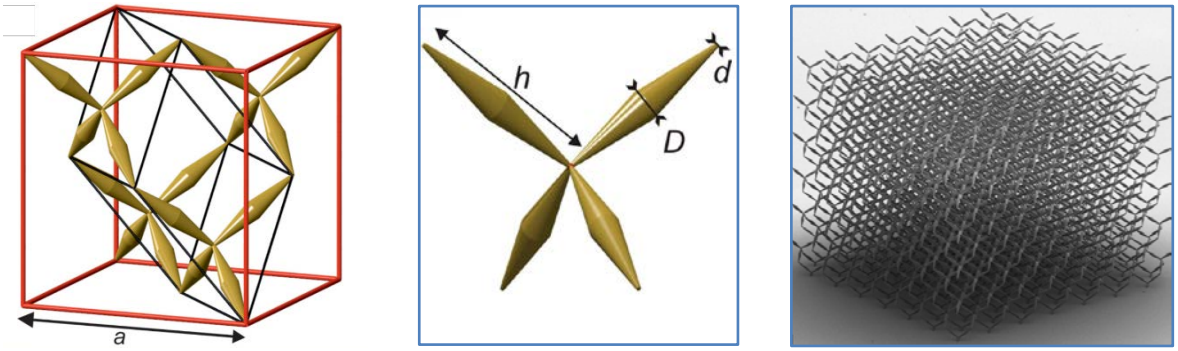

Fig. 1. Concept of conventional rigid-body double-cone pentamode materials [28] based on the Face-Centered Cubic (FCC) lattice.

Since common naturally occurring elastic solids have the Poisson's ratios around 0.3, and $B/G\approx 2$ that indicates B and G are comparable in magnitudes. However, pentamodes are indeed solids but special in making B much large compared to G. When B is ideally finite while $G=0$, the Poisson's ratio of an isotropic pentamode material $v=(3B-2G)/(6B+2G)\approx 0.5$. Hence, the PMMs are also called 'meta-fluids'. In practice, however, when solid microstructures are used to approximate the pentamode behaviour of fluids, it is difficult to make the 3D solid microstructures have an infinitely large bulk modulus while a nearly zero shear modulus. Instead, a relatively large ratio of B/G (e.g. 100-1000) for solid microstructures is realistically attainable. In this case, the transformation elastodynamics is not exactly but still approximately applicable. Conventionally, PMMs were empirically designed by repeatedly testing different dependences of B/G upon different sets of parameters (h, D, d) of the rigid-body double-cone lattice (Fig. 1). A smaller d will gain a larger ratio, but d cannot be infinitely small, as such a tiny rigid-body connection will make manufacturing process extremely challenging and easily fall apart upon a slightest mechanical deformation. Hence, most of current designs for PMMs may be meaningful only in concept not in practice. In this paper, the elastic deformation of the whole microstructures, rather than the highly concentrated deformation from double-cone tips connections within a diamond structures (FCC lattice) (Fig. 2), are utilized to achieve a large ratio of B/G. The PMMs in this research will be designed by the numerical topology optimization method and prototyped by additive manufacturing, as appropriate. The design and manufacturing are critical for the novelty of PMMs.

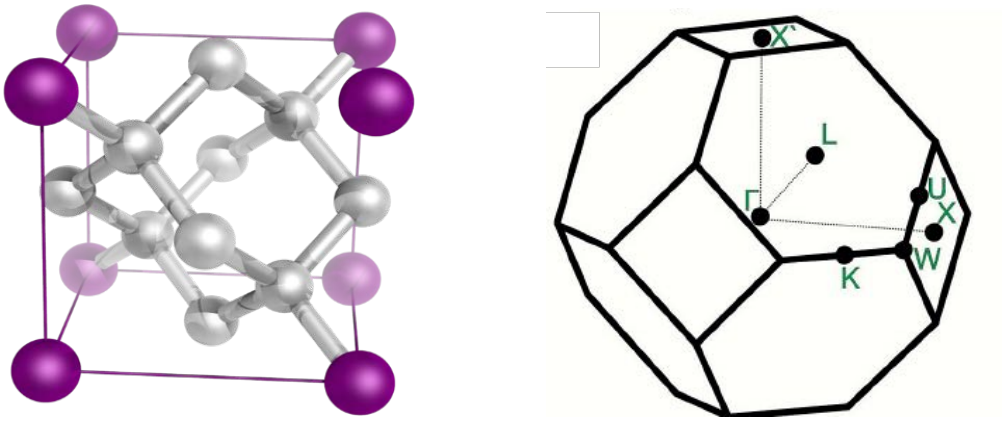

Fig. 2. Concept of diamond-type of lattice (FCC) for pentamode materials

Topology optimization has expanded rapidly as a powerful computational design tool, providing unlimited opportunities for creating novel materials and structures that are stronger and lighter [35, 36]. It is essentially a numerical process to redistribute materials inside a fixed reference domain, until the best material distribution and the corresponding topology are achieved, upon the optimization of a given objective function subject to design constraint(s). It has been a widely recognised computational approach for finding new geometries to enable design innovation of structures, materials, and mechanisms. Over the past three decades, a number of methods have been developed for topology optimization, including the solid isotropic material with penalization (SIMP) [37-40], evolutionary structural optimization (ESO) [41-43], and level set method (LSM) [44-48]. In particular, the SIMP model has been one popular topology optimization method for a range of structural and material designs. Recently, with the rapid development of Additive Manufacturing (AM) techniques, the implementation of structural and mechanical parts with complex geometry is possible [49]. AM removes the limitations of traditional manufacturing processes to remove materials and significantly expands the freedom in topological designs, to allow more intricated shapes and complicated geometries, which often drives the finding of new artificially engineered materials and composites with novel properties.

Topology Optimization has been used to design microstructures of bi-mode metamaterials [50] (2D), and 2D and 3D elastic metamaterial microarchitectures with crystal symmetries [51, 52]. This article is motivated to design three-dimensional solid elastic microstructures with the pentamode properties, to get a realistically achievable large number of the effective bulk modulus over shear modulus. The microstructure is obtained by SIMP-based topology optimization with a single piece of isotropic material, through the overall elastic deformation of the microstructure, and the equivalent property of the microstructure is evaluated by the

numerical homogenization method. The topologically optimized design will be numerically verified, and further optimized (size optimization) within the commercial software ANSYS, and then additive manufacturing technique is used to prototype the optimized pentamode microstructures.

2. Topology Optimization Method

2.1 SIMP material interpolation model

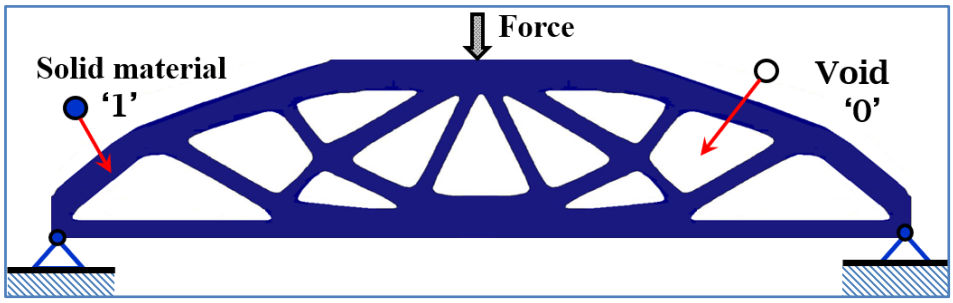

Fig. 3. Topological design for a Messerschmitt-Bölkow-Blohm (MBB) beam

Topology optimization is to seek the optimum distribution of materials by determining the solid ("1") and void ("0") material patterns in the design domain under supports and applied loads [40], as indicated in Fig. 3. However, the optimization deployed in this way in mathematics is a large-scale integer programming problem, to which many gradient-based optimization algorithms cannot be directly applied. As a result, the original 0 and 1 problem is usually relaxed by allowing the material to have intermediate densities in the optimization process. This can usually be achieved by defining an appropriate material interpolation scheme with continuous design variables ranging from 0 to 1, to which many well-founded optimization algorithms such as optimality criterion methods and mathematical programming approaches can be applied. To recover the original binary '1' and '0' material distribution, some simple conditions need to be satisfied [53] to push the intermediate element densities towards its prescribed 1 and 0 bounds. A meaningful solution can be further guaranteed by eliminating numerical instabilities such as mesh-dependency and checkerboards [54]. The SIMP based methods have got popularity due to its conceptual and practical simplicity.

Numerically, SIMP is described by a nonlinear density-stiffness interpolation, which denotes the dependency of elemental pseudo densities upon material properties [53, 55]. For each element, its practical modulus during the numerical implementation is variable, which can be expressed as

$$E(x) = x_j^p E_0 \tag{1}$$

where E_0 represents modulus of solid material. The design variable x_j are relaxed to allow intermediate values within its two bounds ($x_{\min} \le x_j \le 1$) during the optimization. In this way, the original design optimization problem, with discrete '1' and '0' design variables, is transformed into an optimization problem with continuous design variables ranging from 0 to 1. The final design optimization problem can then be solved by mathematical programming algorithms, based on the sensitivities of the objective and constraint functions. To make the continuous design after the relaxation approximate the original '0' and '1' material distribution, the penalty exponent of the SIMP model is usually advised to be *p*=3, in order to push intermediate element densities towards its prescribed lower and upper bounds.

2.2 Numerical homogenization method

The numerical homogenization method [1, 56] has been widely used to evaluate the effective properties of microstructures, subject to the satisfaction of two assumptions: (1) The geometrical dimensions of the unit cell (e.g. microstructure) are sufficiently small compared to the bulk material; and (2) the microstructures are periodically rather than randomly distributed within the macrostructure.

For a 3D microstructure with linear elastic material, the macroscopic effective elasticity tensor of the microstructure can be calculated by:

$$C_{ijkl}^H = \frac{1}{|\Omega_m|}\int_{\Omega_m}\left(\varepsilon_{pq}^{0(ij)} - \varepsilon_{pq}\left(\chi^{ij}\right)\right)C_{pqrs}\left(\varepsilon_{rs}^{0(kl)} - \varepsilon_{rs}\left(\chi^{kl}\right)\right)d\Omega_m \quad \left(i,j,k,l = 1,2,\ldots,d\right) \tag{2}$$

where $|\Omega_m|$ refers to the volume of the 3D microstructure, and *C* is the elasticity tensor of the solid material. ε^0 is the applied strain field with six linearly independent unit strains, and ε indicates the locally varying strain field within the microstructure. Hence, the corresponding unknown displacement field χ^{kl} induced by the applied initial strain field can be obtained by solving the following linear elasticity equilibrium equation using the finite element method:

$$\int_{\Omega_m}\varepsilon_{ij}\left(v^{kl}\right)C_{ijpq}\varepsilon_{pq}\left(\chi^{kl}\right)d\Omega_m = \int_{\Omega_m}\varepsilon_{ij}\left(v^{kl}\right)C_{ijpq}\varepsilon_{pq}^{0(kl)}d\Omega_m,\ \forall v^{kl} \in \bar{\mathrm{U}}\left(\Omega_m\right) \tag{3}$$

where *v* is the virtual displacement in the microstructure, belonging to the space that includes all the kinematically admissible displacements in Ω_m.

Under the assumption of periodicity, the displacement field of the base cell subjected to a given strain ε^0 can be expressed as the sum of macro displacement field and periodic fluctuation displacement field:

$$u_i = \varepsilon_{ij}^0 y_j + u_i^* \tag{4}$$

Where u_i^* is the periodic fluctuation displacement field in macroscopic materials, which is unknown and difficult to solve. Therefore, the above formula can not be applied to the microstructure directly. It is necessary to transform the implicit boundary conditions into explicit ones. Based on the Eq. (4), the displacement field of the boundary in all normal directions of the microstructure can be solved as follows:

$$\begin{aligned} u_i^{k+} &= \varepsilon_{ij}^0 y_j^{k+} + u_i^* \\ u_i^{k-} &= \varepsilon_{ij}^0 y_j^{k-} + u_i^* \end{aligned} \tag{5}$$

Where $k+$ and $k-$ represents the normal direction of two opposite boundaries in the structure, the sign '+' indicates the same direction with the coordinate axis, and the sign '-' indicates the opposite direction to the coordinate axis. Based on the Eq. (5), the unknown periodic fluctuation displacement field in microstructure can be eliminated by subtraction:

$$u_i^{k+} - u_i^{k-} = \varepsilon_{ij}^0 (y_j^{k+} - y_j^{k-}) = \varepsilon_{ij}^0 \Delta y_j^k \tag{6}$$

Where $\varepsilon_{ij}^0 \Delta y_j^k$ represents the periodic boundary conditions in the microstructure, and Δy_j^k can be used to represent the scale value in the normal direction of the microstructure. It can be seen that the explicit periodic boundary conditions in the Eq. (6) can be directly applied to the boundary area, boundary line and vertex of the material microstructure.

3. Topology Optimization Formulation

Pentamodes are special in that they can uncouple compression and shear waves by making the bulk modulus (B) extremely large when compared to the shear modulus (G). When B is ideally infinitely large, and G is close to zero, the Poisson's ratio v=(3-2(G/B))/(2(G/B)+6)=0.5. In this case, a diagonalized elasticity tensor for a 3D isotropic pentamode material will have 5 diagonal elements out of 6 are zero. The pentamode materials under this situation are a kind perfect homogeneous pentamode materials, like the isotropic fluids that will flow away. However, as noted in the work by Milton and Cherkaev [27], pentamode materials can be approximated by specially designed three-dimensional (3D) solid microstructures. The artificially engineered 3D pentamode metamaterials, the counterpart of bimode metamaterials in two dimensions, will have effective

shear modulus with the magnitudes smaller than their effective bulk modulus in orders, which indicates their effective Poisson's ratio will be close to 0.5 but smaller than the upper limit.

As indicated by Fig. 4, on one hand, for a three-dimensional isotropic pentamode material, when the shear modulus G becomes very small compared to the bulk modulus B, and B/G is a large number and the Poisson's ratio approaches 0.5. On the other hand, for a three-dimensional isotropic auxetic material [57], the ratio of B/G gets very small, and the Poisson's ratio approaches −1.0. Therefore, a pentamode material can be regarded as an 'anti-auxetic' [30]. In this study, the design of solid pentamode materials will be transformed into the design of its effective Poisson's ratio close to o.5 under appropriate constraints.

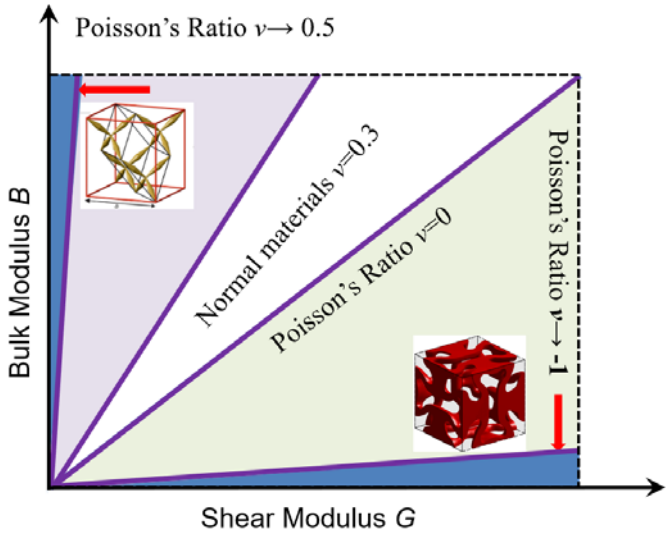

Fig. 4. Schema to indicate relationship of Poisson's ratio, Bulk and Shear modulus

In most up-to-date designs, as denoted in Fig. 4, the 3D solid pentamode microstructures are given by a diamond lattice corresponding to face centred-cubic (FCC) lattice constant 'a', as shown in Fig. 1. The lattice consists of rigid-body double-cone elements connected to each other only by their point-like tips. In this section, inspired by the rigid-body diamond lattice, topology optimization technique with SIMP model is applied to generate 3D pentamode microstructures with isotropic materials. The optimization is formulated to make the effective Poisson's ratio of the microstructure close to 0.5, so that the ratio B/G of the microstructure is sufficiently large. The elasticity tensor for such micro-structured materials has five smaller eigenvalues and only one eigenvalue that is comparably very large. Hence, the design problem is formulated to let the effective Poisson's ratio of the pentamode microstructure close to the given property (0.5), under appropriate constraints.

For three-dimensional isotropic elastic materials, the elasticity tensor can be given by

$$C=\begin{bmatrix} C_{11} & C_{12} & C_{13} & 0 & 0 & 0 \\ C_{21} & C_{22} & C_{23} & 0 & 0 & 0 \\ C_{31} & C_{32} & C_{33} & 0 & 0 & 0 \\ 0 & 0 & 0 & C_{44} & 0 & 0 \\ 0 & 0 & 0 & 0 & C_{55} & 0 \\ 0 & 0 & 0 & 0 & 0 & C_{66} \end{bmatrix} \tag{7}$$

The symmetric conditions are given by

$$C_{11}=C_{22}=C_{33} \tag{8}$$

$$C_{44}=C_{55}=C_{66} \tag{9}$$

$$C_{12}=C_{21}=C_{13}=C_{31}=C_{23}=C_{32} \tag{10}$$

The isotropy conditions are

$$C_{11}-C_{12}=2C_{44} \tag{11}$$

Considering the above conditions, the elasticity tensor then changes to the following form:

$$C=\begin{bmatrix} C_{11} & C_{12} & C_{12} & 0 & 0 & 0 \\ C_{12} & C_{11} & C_{12} & 0 & 0 & 0 \\ C_{12} & C_{12} & C_{11} & 0 & 0 & 0 \\ 0 & 0 & 0 & (C_{11}-C_{12})/2 & 0 & 0 \\ 0 & 0 & 0 & 0 & (C_{11}-C_{12})/2 & 0 \\ 0 & 0 & 0 & 0 & 0 & (C_{11}-C_{12})/2 \end{bmatrix} \tag{12}$$

According to the elasticity theory we have

$$C_{11}=\frac{E(1-\upsilon)}{(1+\upsilon)(1-2\upsilon)} \quad \text{and} \quad C_{12}=\frac{E(1-\upsilon)}{(1+\upsilon)(1-2\upsilon)}\frac{\upsilon}{1-\upsilon} \tag{13}$$

Substitute them into Eq. (12), the elasticity tensor has the following form

$$C=\frac{E}{(1+\upsilon)(1-2\upsilon)}\begin{bmatrix} 1-\upsilon & \upsilon & \upsilon & 0 & 0 & 0 \\ \upsilon & 1-\upsilon & \upsilon & 0 & 0 & 0 \\ \upsilon & \upsilon & 1-\upsilon & 0 & 0 & 0 \\ 0 & 0 & 0 & (1-2\upsilon)/2 & 0 & 0 \\ 0 & 0 & 0 & 0 & (1-2\upsilon)/2 & 0 \\ 0 & 0 & 0 & 0 & 0 & (1-2\upsilon)/2 \end{bmatrix} \tag{14}$$

When the Poisson's ratio is close to 0.5, we can find $C_{11}=C_{12}\rightarrow+\infty$. At the same time, in terms of Eq. (9), we have $C_{44}=C_{55}=C_{66}\rightarrow 0$. If we regard $E/((1+\upsilon)(1-2\upsilon))$ as a large constant compared to C_{44}, C_{55} and C_{66}, such

as 1, the elasticity tensor can be re-written as follows:

$$C=\begin{bmatrix}1&1&1&0&0&0\\1&1&1&0&0&0\\1&1&1&0&0&0\\0&0&0&0&0&0\\0&0&0&0&0&0\\0&0&0&0&0&0\end{bmatrix} \tag{15}$$

In the above Equation, we can find its eigenvector is $[3\ 0\ 0\ 0\ 0\ 0]^{T}$, in which 5 eigenvalues are zero and only one is non-zero. At the same time, we can find that the bulk modulus B=1 while a vanishing shear modulus G=0, so that their ratio $B/G\rightarrow+\infty$. The above elasticity theory shows that when the Poisson's ratio of isotropic elastic materials is close to 0.5, the solid materials can be approximately regarded as pentamode materials.

Based on the SIMP model, the optimization formulation for the pentamode materials can be defined by

$$\begin{cases} Min: \quad c=0.5-\upsilon \\ Subject\ to: K\chi^{ij}=f^{ij} \\ \qquad C_{11}=C_{22}=C_{33} \\ \qquad C_{44}=C_{55}=C_{66} \\ \qquad C_{12}=C_{21}=C_{13}=C_{31}=C_{23}=C_{32} \\ \qquad C_{11}-C_{12}=2C_{44} \\ \qquad \sum_{e=1}^{N_e}(x_e v_e)=v_f v_0 \\ \qquad 0<x_{\min}\le x_e\le 1 \end{cases} \tag{16}$$

where N_e is used to indicate the number of elements, v_e and v_0 are the volume of each element and the total volumes of the design domain. v_f is the given volume ratio of the design. The constraints Eqs. (5)-(7) are used to denote the symmetry of the central plane and the diagonal plane of the microstructure, while the constraint Eq. (11) represents the isotropy of the microstructure.

In this paper, the effective Poisson's ratio of the microstructure is not recommended as the objective function based on the expeience and recommendation of the literature [13, 15, 57, 58]. This study uses the following formulation as an alternative objective function in the optimization:

$$\begin{cases} Min: \ c^* = -C_{12} \\ Subject\ to: K\chi^{ij} = f^{ij} \\ \qquad C_{11} = C_{22} = C_{33} \\ \qquad C_{44} = C_{55} = C_{66} \\ \qquad C_{12} = C_{21} = C_{13} = C_{31} = C_{23} = C_{32} \\ \qquad C_{11} - C_{12} - 2C_{44} = 0 \\ \qquad \sum_{e=1}^{N_e} (x_e v_e) = v_f v_0 \\ \qquad 0 < x_{\min} \le x_e \le 1 \end{cases} \tag{17}$$

The Zener ratio parameter β [59] is used to indicate the anisotropy of the microstructure. When β is closer to 1, the effective properties of the microstructure are closer to isotropy.

$$\beta = \frac{C_{11} - C_{12}}{2C_{44}} \tag{18}$$

4. Topological design and discussions

In this section, the SIMP-based topology optimization approach, with the numerical homogenization method [15], is used to implement the computational design of pentamode materials. The Young's modulus and Poisson's ratio for the base material are assumed to be $E = 1$ and $\upsilon = 0.3$. In order to capture fine structural features under a very small volume constraint such as 0.01, the initial guess of the micro-lattice structure (Fig. 5) is meshed by 150×150×150 elements. In the SIMP model, the penalty parameter is p=3 and the filtering radius is 1.5 in the sensitivity method [39]. The MMA optimization algorithm is used [60]. The optimization results and the final topology for the microstructure are given in the following figures (Figs. 6-8).

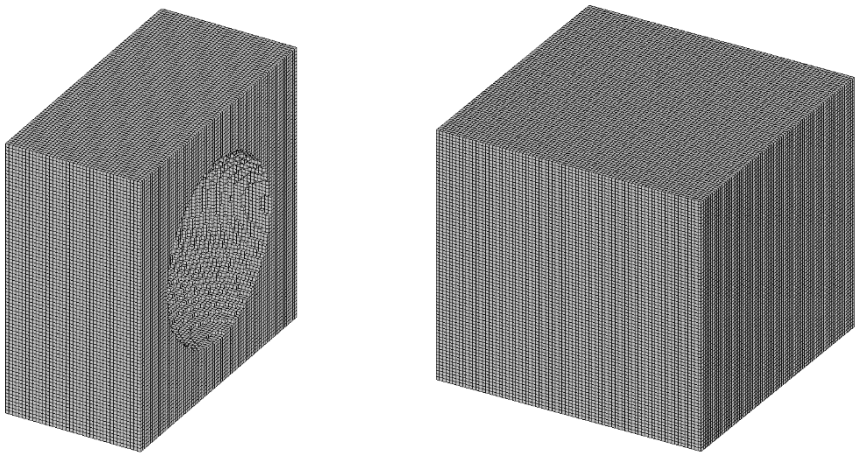

Fig. 5. Initial design domain of the micro-lattice structure (left-half, right-whole)

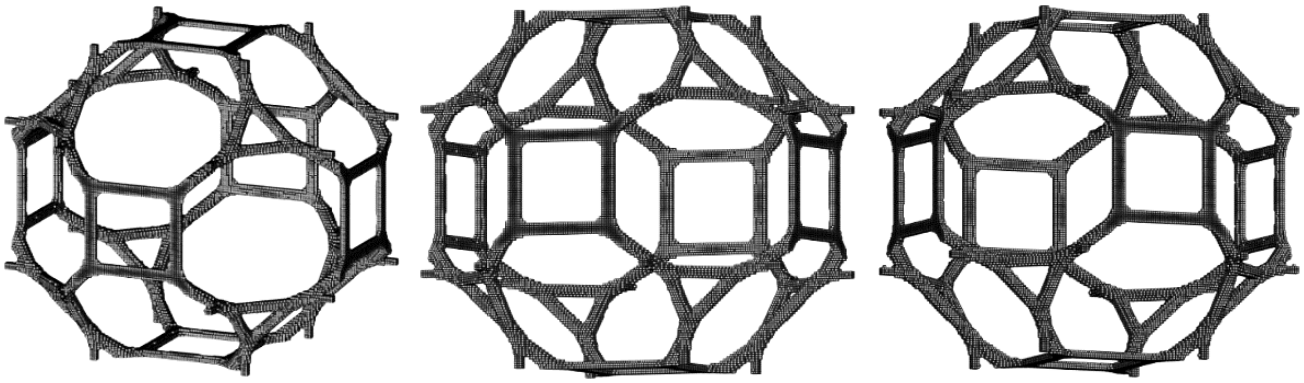

Fig. 6. Topological design of pentamode microstructure from different aspects

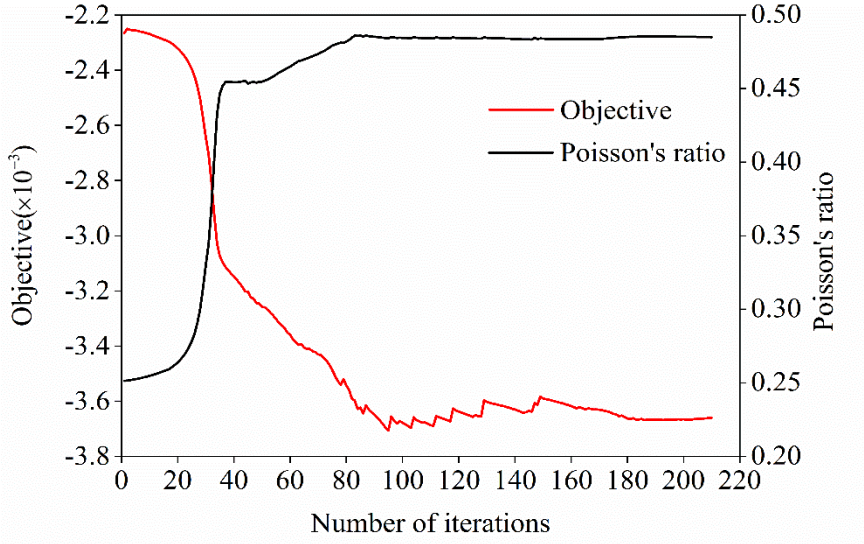

Fig. 7. Plots of the objective function and Poisson's ratio

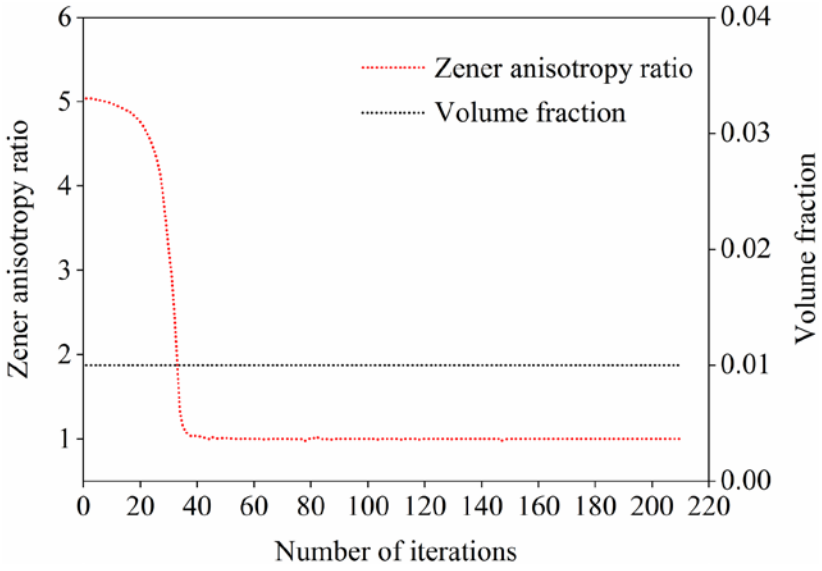

Fig. 8. Plots of Zener anisotropy ratio and volume fraction

In Fig. 6, it can be found that the topological design of the microstructure satisfies symmetrical conditions, with respect to the central plane and the diagonal plane. From the results of the optimized microstructure, we can find that the eigenvalues of the effective elasticity tensor is [0.001868 3.8e-05 3.8e-05 1.90e-05 1.90e-05 1.90e-05]^{T}, where only one eigenvalue is large compared to five of the values, and the largest value 0.001868 is about 50-100 times of the small ones. It can also be seen that the ratio B/G of the bulk modulus (B) over the shear modulus (G) is about 33, and the corresponding Poisson's ratio is 0.485. Hence, the results from three different aspects demonstrate that the optimized microstructure meets all the characteristics of the pentamode material. The proposed optimization formulation is reasonable to achieve the pentamode design of microstructures. When the effective Poisson's ratio under isotropy and symmetry conditions is close to 0.5 (Figs. 7-8), the solid 3D microstructure approximated shows the features of the pentamode materials. The elasticity tensor corresponds to the optimized design is given as follows:

$$C^{*}=10^{-3}\begin{bmatrix} 0.648 & 0.610 & 0.610 & 0.000 & 0.000 & 0.000 \\ 0.610 & 0.648 & 0.610 & 0.000 & 0.000 & 0.000 \\ 0.610 & 0.610 & 0.648 & 0.000 & 0.000 & 0.000 \\ 0.000 & 0.000 & 0.000 & 0.019 & 0.000 & 0.000 \\ 0.000 & 0.000 & 0.000 & 0.000 & 0.019 & 0.000 \\ 0.000 & 0.000 & 0.000 & 0.000 & 0.000 & 0.019 \end{bmatrix} \tag{19}$$

It is noted that the lattice structure given in Fig. 1 is a conventional typical design based on multi-rigid body concept, which gains its pentamode behavior dominantly through the highly localized deformation from the tiny connections of double-cone tips. It is useful in concept, but it is easily subject to breakage in practice.

The micro-lattice structure in Fig. 6 is the new design obtained through the proposed topology optimization method. It achieves pentamode behaviour by the overall elastic deformation of the entire microstructure, rather than the tiny rigid-body double-cone connections which often makes the manufacturing process extremely hard and will be easily broken upon deformation of the lattice structure.

5. Evaluation of pentamode microstructures using ANSYS

5.1 A new implementation of numerical homogenization method

In [61], there is a new implementation numerical homogenization method to evaluate effective properties for three-dimensional periodic microstructures. This method can be applied to any three-dimensional microstructures with different finite elements (e.g., beam elements), to evaluate the effective properties of the

microstructure by fully making use of commercial software tools, such as ANSYS.

Firstly, the six unit strain fields $\varepsilon^{0(ij)}$ are applied to the microstructure to get the corresponding nodal displacements $\chi^{0(ij)}$. The displacement will be applied to ANSYS model for finite element analysis to generate the nodal forces f^{ij} (f^{kl}) of the microstructure. Then after another finite element analysis, ANSYS can directly output the displacement field χ^{ij} subject to periodic boundary conditions, due to the given unit strain field. Applying the χ^{ij} to the ANSYS microstructure for a third finite element analysis, we can get nodal reaction forces $f^{*(kl)}$. Finally, we can calculate the effective elasticity tensor as follows:

$$C_{ijkl}^{H}=\frac{1}{\left|\Omega_m\right|}\int_{\Omega_m}\left(\left(\chi^{0(ij)}-\chi^{ij}\right)^{T}\left(f^{kl}-f^{*(kl)}\right)\right)d\Omega_m \tag{20}$$

5.2 Size optimization of the microstructure using ANSYS

The SIMP topology optimization method results in designs often with elements having intermediate densities. How to appropriately process those elements will particularly impact the performance of microstructures for ultra-bulk modulus and shear modulus but ultra-lightweight with low densities. Hence, this section will make use of the structural skeleton (Fig. 9) obtained from the above topological optimization. The skeleton is constructed by extracting the key points' coordinate manually. Then, under the given topology, the commercial software ANSYS will be used to parameterize the topologically optimized design and develop the finite element model for the solid 3D pentamode material. The numerical homogenization method is still used to predict the effective properties of the parameterized microstructure by ANSYS.

In ANSYS the skeleton of the topological design will be kept unchanged, but different geometrical sizes of the micro-lattice structure will be selected to demonstrate their effects on the pentamode properties. ANSYS will be used to conduct size optimization for pentamode microstructure through its embedded optimizer, and beam elements are used to mesh the skeleton structure with different equivalent cross-sectional areas. The objective function is to maximize the ratio of bulk modulus with respect to the shear modulus, subject to the constraints of Poisson's ratio (no less than that of the microstructure before the optimization) and isotropy, and here the design variables are the microstructural dimensions such as the sizes A1 to A5 given in Fig. 10(b).

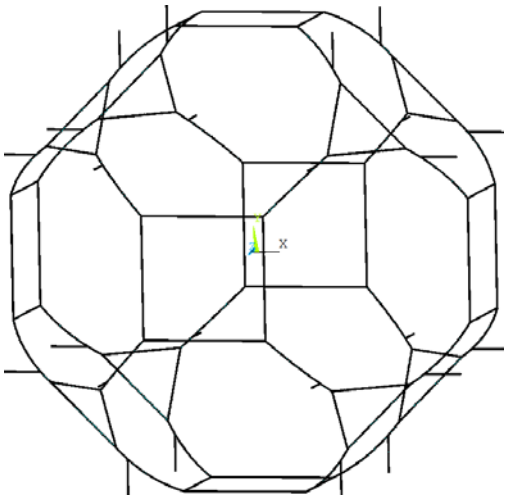

Fig. 9. Skeleton of the topologically optimized microstructure

(1) The ANSYS results with geometric size 0.4mm

Firstly, the member radius of the microstructure is assumed to be 0.4mm, and the volume ratio is 0.0161. The finite element mesh is given in Fig. 10(a), and its corresponding geometry is shown in Fig. 10(b). After optimization, The effective elasticity tensor evaluated by ANSYS is given in Eq. (21). The Zener anisotropy ratio of the elasticity tensor is improved from 1.09 to 1.01, the Poisson's ratio increase from 0.478 to 0.480, and the ratio B/G of the bulk modulus B over the shear modulus G is improved from 24 to 25. The eigenvalue vector of the elasticity tensor related to the optimized micro-lattice is [0.006293 1.68e-04 1.68e-04 8.34e-05 8.34e-05 8.34e-05]^T. The optimized micro-lattice still satisfies the fundamental properties of a solid 3D microstructure.

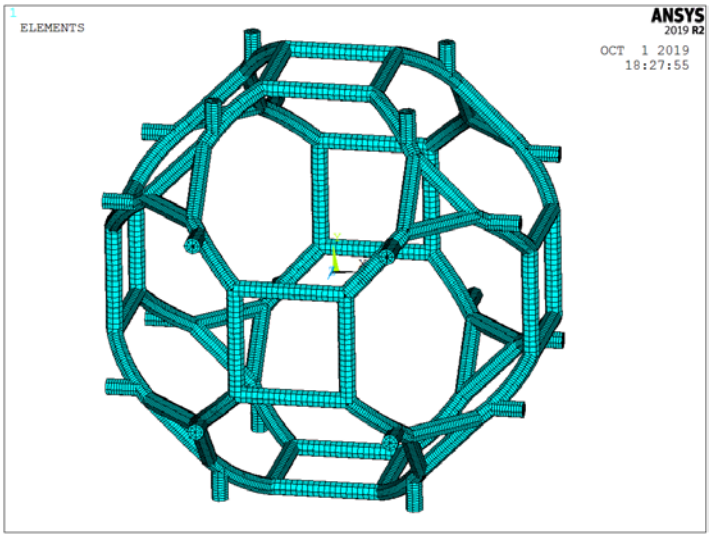

Fig. 10(a) Finite element model

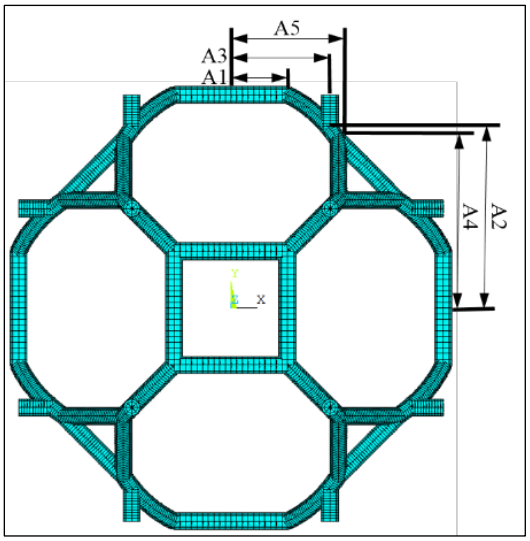

Fig. 10(b) Sizes of the model

$$C^* = 10^{-3}\begin{bmatrix} 2.20979 & 2.04145 & 2.04145 & 0 & 0 & 0 \\ 2.04145 & 2.20979 & 2.04145 & 0 & 0 & 0 \\ 2.04145 & 2.04145 & 2.20979 & 0 & 0 & 0 \\ 0 & 0 & 0 & 0.08336 & 0 & 0 \\ 0 & 0 & 0 & 0 & 0.08336 & 0 \\ 0 & 0 & 0 & 0 & 0 & 0.08336 \end{bmatrix} \tag{21}$$

(2) The ANSYS results with geometric size 0.3mm

Secondly, when the geometrical size of the microstructure is changed to 0.3mm, and the volume ratio is 0.0091. The finite element mode and its corresponding geometry are shown in Fig. 11(a) and Fig. 11(b). After optimization, the elasticity tensor is expressed in Eq. (22). the Zener parameter relative to the elasticity tensor drops from 1.12 to 1.01, the effective Poisson's ratio increase from 0.486 to 0.488, and the ratio B/G is improved from 40 to 43. The eigenvalue vector of the elasticity tensor related to the optimized micro-lattice is $[0.003408\ 5.34e\text{-}05\ 5.34e\text{-}05\ 2.65e\text{-}05\ 2.65e\text{-}05\ 2.65e\text{-}05]^T$.

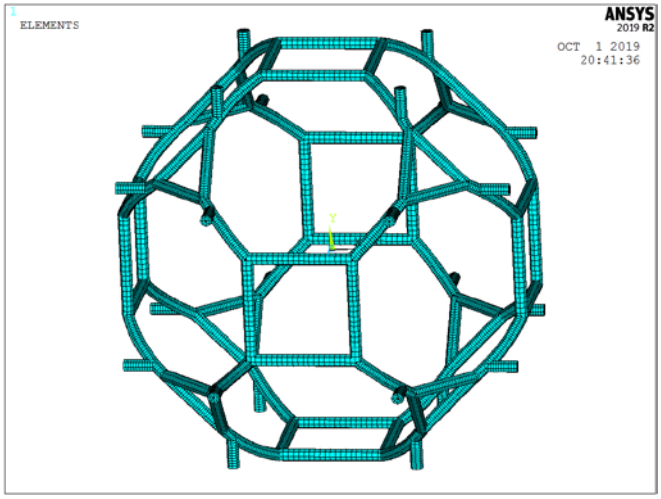

Fig. 11(a) Finite element model

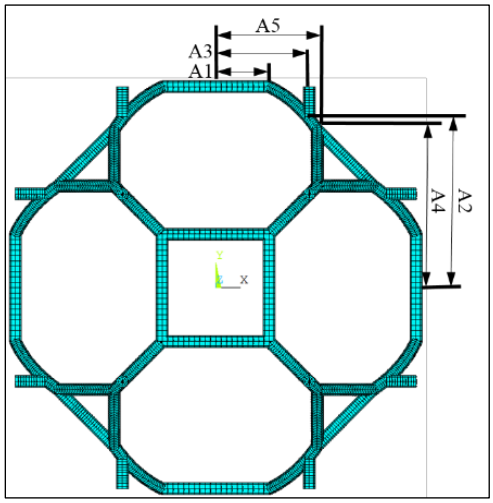

Fig. 11(b) Sizes of the model

$$C^* = 10^{-3}\begin{bmatrix} 1.17159 & 1.11818 & 1.11818 & 0 & 0 & 0 \\ 1.11818 & 1.17159 & 1.11818 & 0 & 0 & 0 \\ 1.11818 & 1.11818 & 1.17159 & 0 & 0 & 0 \\ 0 & 0 & 0 & 0.02647 & 0 & 0 \\ 0 & 0 & 0 & 0 & 0.02647 & 0 \\ 0 & 0 & 0 & 0 & 0 & 0.02647 \end{bmatrix} \tag{22}$$

(3) The ANSYS results with geometric size 0.2mm

Thirdly, when the geometrical size of the microstructural bar members is changed to 0.2mm, the volume ratio of the microstructure is about 0.0042, the finite element model and its geometry are displayed in Fig. 12(a) and Fig. 12(b). After optimization, the calculated effective elasticity tensor by ANSYS is given in the Eq. (23).

It can be seen that the Zener ratio of anisotropy of the optimized microstructure is still 1.01 (1.14 before optimization), the effective Poisson's ratio increases from 0.491 to 0.494, and the ratio *B*/*G* of the bulk modulus B and the shear modulus G is improved from 81 to 84. The eigenvalue vector of the elasticity tensor is [0.001311 1.05e-05 1.05e-05 5.19e-06 5.19e-06 5.19e-06]^{T}.

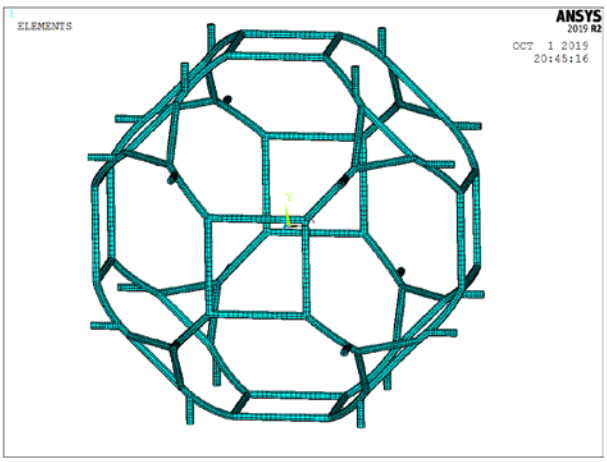

Fig. 12(a) Finite element model

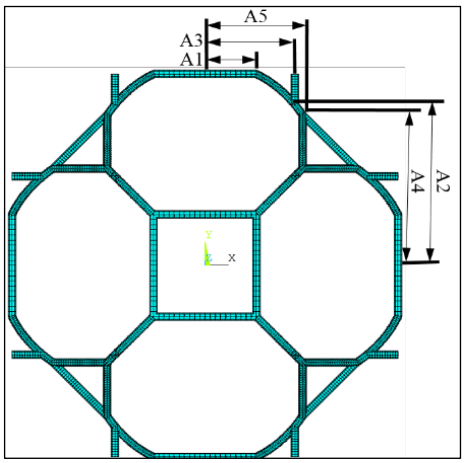

Fig. 12(b) Sizes of the model

$$C^{*}=10^{-3}\begin{bmatrix} 0.44393 & 0.43343 & 0.43343 & 0 & 0 & 0 \\ 0.43343 & 0.44393 & 0.43343 & 0 & 0 & 0 \\ 0.43343 & 0.43343 & 0.44393 & 0 & 0 & 0 \\ 0 & 0 & 0 & 0.00519 & 0 & 0 \\ 0 & 0 & 0 & 0 & 0.00519 & 0 \\ 0 & 0 & 0 & 0 & 0 & 0.00519 \end{bmatrix} \tag{23}$$

(4) The ANSYS results with geometric size 0.1mm

Finally, if we change the bar radius of the microstructure to 0.1mm, the volume ratio of the microstructure is about 0.0011, the finite element model and its geometry are displayed in Fig. 13(a) and Fig. 13(b). After optimization, the effective elasticity tensor calculated by ANSYS is shown in Eq. (24). The Zener anisotropy ratio is 1.01 (1.08 before optimization), the effective Poisson's ratio of the microstructure increase from 0.496 to 0.498, and the ratio *B*/*G* of the bulk modulus B and the shear modulus G related to the optimized micro-lattice is improved from 207 to 212. The eigenvalue vector of the elasticity tensor is [2.53e-4 8.10e-07 8.10e-07 4.00e-07 4.00e-07 4.00e-07]^{T}.

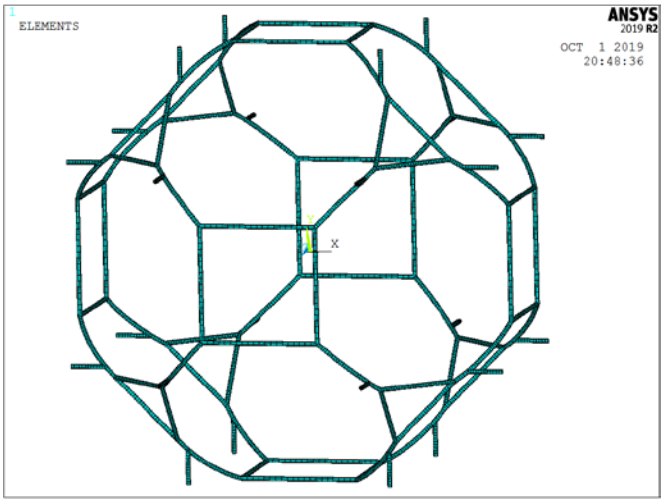

Fig. 13(a) Finite element model

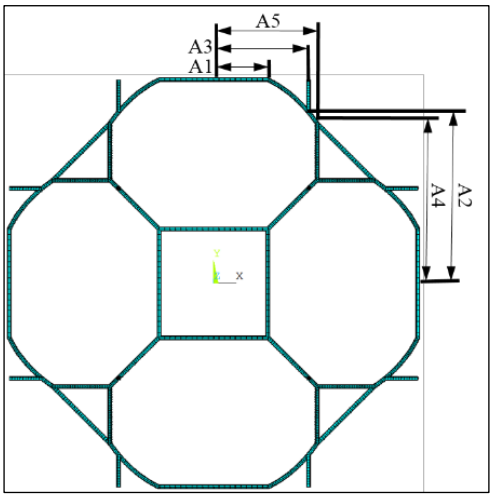

Fig. 13(b) Sizes of the model

$$C^* = 10^{-3}\begin{bmatrix} 0.08497 & 0.08416 & 0.08416 & 0 & 0 & 0 \\ 0.08416 & 0.08497 & 0.08416 & 0 & 0 & 0 \\ 0.08416 & 0.08416 & 0.08497 & 0 & 0 & 0 \\ 0 & 0 & 0 & 0.00040 & 0 & 0 \\ 0 & 0 & 0 & 0 & 0.00040 & 0 \\ 0 & 0 & 0 & 0 & 0 & 0.00040 \end{bmatrix} \quad (24)$$

As discussed above, the size optimization results under 4 different cases are summarized in Table 1. From the table, we can find that the worst pentamode microstructure is the design with the beam diameter d=0.4mm, while the best pentamode microstructure is the design with the beam diameter d=0.1mm. When the beam diameter is changing from 0.4mm to 0.1mm, the ratio (B/G) of the effective bulk modulus over the shear modulus increases from 75 to 635, and the effective Poisson's ratio is increased from 0.480 to 0.498. If the diameter is getting smaller and smaller, the B/G magnitude will be larger and larger (e.g. over 1000), and Poisson's ratio υ will gradually approach to 0.5, with a better performance for mimicking liquid by the solid microstructures. Hence, the pentamode microstructure in this study can be applied to simulate the behaviour of the liquid for transformation of elastodynamics. A smaller beam diameter is beneficial to achieve a much larger ratio of B/G, but the manufacturing will get difficult. The latest additive manufacturing technique such as selective laser melting (SLM) can be used to produce components with metallic materials, but the topologically optimized 3D microstructures with a diameter less than 0.1mm (0.05mm) are still challenging.

Table 1. Properties corresponding to different parameters and diameters (unit mm)

Parameters	ET	d	A1	A2	A3	A4	A5	***B/G***	*Z*	υ

Topology Optimization	Solid	----	1.33	4.20	2.33	3.93	2.53	**37**	1.01	**0.486**
Size Optimization	Beam	**0.4**	1.34	4.27	2.27	3.74	2.57	**25**	1.01	**0.480**
Size Optimization	Beam	**0.3**	1.34	4.28	2.26	3.67	2.60	**43**	1.01	**0.488**
Size Optimization	Beam	**0.2**	1.33	4.25	2.31	3.89	2.53	**84**	1.01	**0.494**
Size Optimization	Beam	**0.1**	1.35	4.20	2.33	3.95	2.56	**212**	1.01	**0.498**

5.3 Stress analysis of the microstructure using ANSYS

Since the stress level inside the microstructure depends on its boundary conditions in practice, it is not possible to test all the different cases. Here, only one case is used to indicate different stress distributions when the pentamode microstructure is subjected to compressive and shear deformations. The microstructural array with 4×4×4 microstructures (Fig. 14) is loaded under compressive and shear loads, respectively. In order to ensure the fairness of the comparison between compression and shear loading, the loads applied on each node under the two conditions are both 1N. The difference is that the direction of the compressive loads is normal to the external surface, while the direction of the shear loads is along the plane direction of external surface. Two cells which have the same shapes are picked out to show the difference between the compressive (Fig. 15a) and shear (Fig. 15b) stresses. From the results, the maximal stress under compression is 2.73MPa while the maximal stress under shear loading is 24.83MPa. It is clearly to demonstrate that the pentamode microstructure has a high shear stress level than compression stress level and is easily damaged under shear deformation.

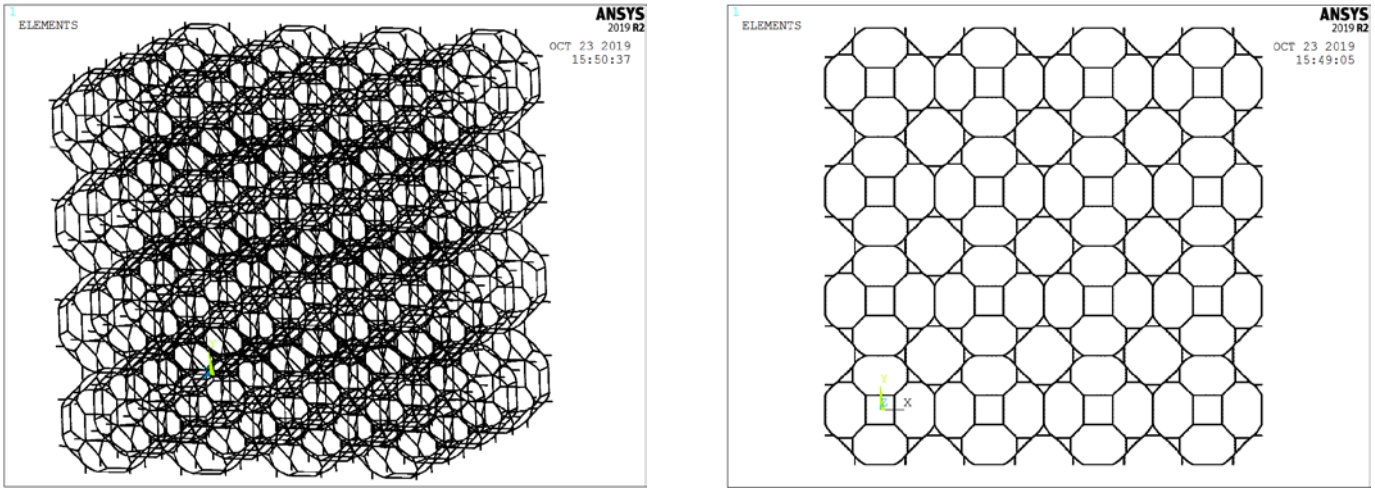

Fig 14. Microstructural array (4×4×4 microstructures) for stress analysis

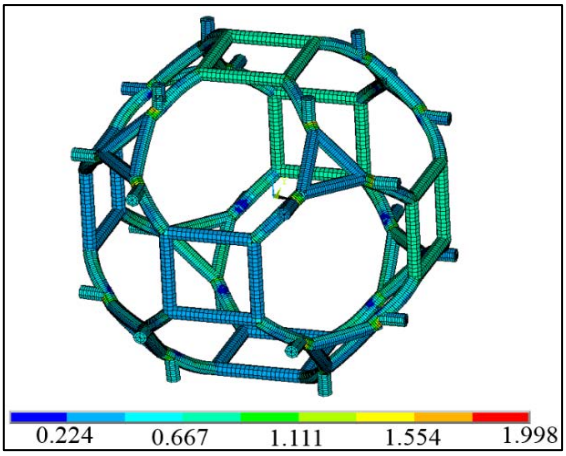

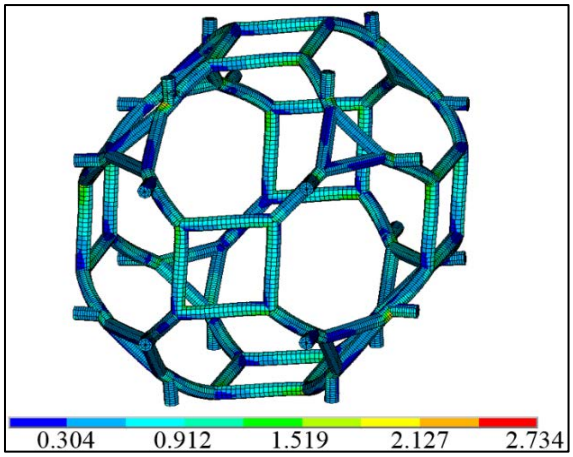

(a) Stress distribution under compressive loading

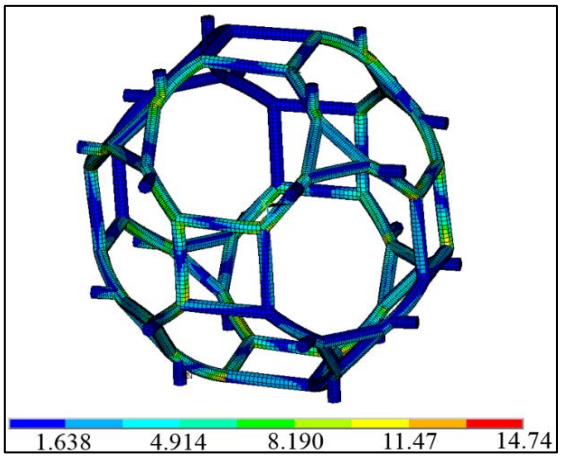

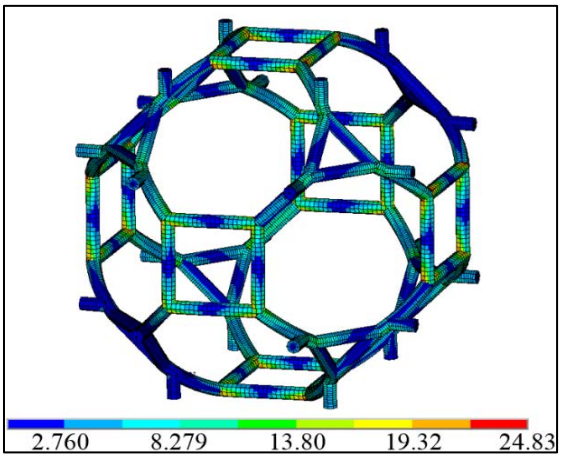

(b) Stress distribution under shear loading

Fig. 15. Von Mises Stress distribution

5.3 Prototype of metallic pentamode microstructures using SLM technique.

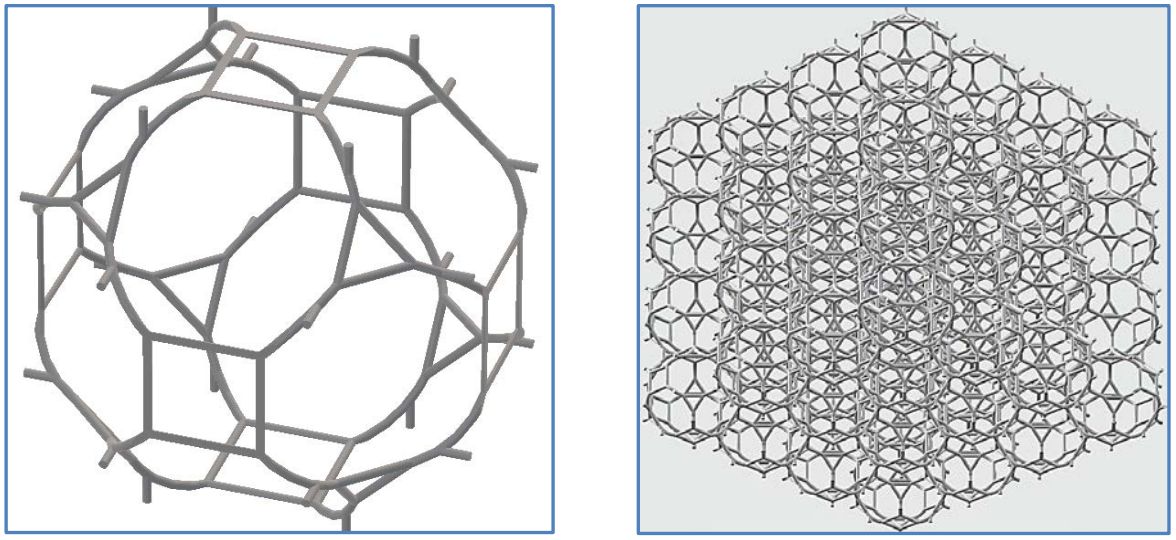

Fig. 16. Microstructure with 0.4 mm diameter, and its 4×4×4=64 array in STL files

AM technologies [62] for producing metallic cellular composites with various microstructures typically include selective laser melting (SLM), selective electron beam melting (SEBM) and laser metal deposition (LMD), also called direct laser fabrication (DLF). Their common feature is to locally melt a powder layer and then rapidly solidified. As a tool-free, cost-efficient and computational manufacturing approach, AM offers many benefits that are changing conventional industrial paradigm in manufacturing for various sectors such as aerospace, automotive, energy, and medical engineering.

Selective laser melting (SLM) [63], a particular rapid prototyping technique that employs high-power laser beam to melt and fuse metallic powders, can manufacture high relative density metal parts through a layer-by-layer process. SLM, with other names like the direct selective laser sintering (DSLS), direct metal laser sintering (DMLS) and LaserCusing, has been proven to produce near net-shape parts. It is applicable to a wide range of materials including metallic materials, e.g. copper, aluminum, tungsten and their alloys, as well as ceramic and composite materials. Due to rapid cooling rates and directional solidification, the additively manufactured metallic microstructures with effective properties may be different from their conventional counterparts. It is important to test and characterize their topologically optimized properties in lab. However, this paper is more focused on computational design of 3D solid pentamode microstructures using topology optimization. Hence, the SLM technique is only used to demonstrate that the topologically optimized pentamode materials (Fig. 16) can be fabricated using up-to-date additive manufacturing technologies. The details for computational manufacturing by AM, as well as in-lab testing and property characterization of more advanced optimized pentamode cellular composites will be published soon with different focuses.

Table 2. Parameters for SLM printing

Parameters	Laser power	Scanning speed	Hatch spacing	Thickness	Remarks
	360 W	1050 mm/s	0.09 mm	0.03 mm	
Support	No				Overhang
Equipment	EOS 290				
Materials	AlSi10Mg				

The printing parameters are given in the following table (Table 2). The structure consists of periodic microstructures with side length a=10 mm, and each microstructure has a volume of $10 \times 10 \times 10$ mm^3. The whole specimen is therefore cubic and occupies a total nominal volume of 40 mm × 40 mm × 40 mm^3. As shown in Fig. 17, we can find that there are many cantilever-style parts, also called overhang struts, in the

structure. If the cantilever parts are too long, the cantilever struts are prone to collapse. If the support structure is used, the internal support is difficult to remove and hence the whole structure is not easy to form near net shape. Hence, the lighter aluminum alloy rather than the heavier titanium alloy is used in the process of the SLM printing. The density of the aluminum alloy is low (ρ = 2.7 g/cm^3), and the struts can therefore be supported by the powder bed in the melting state and the printed structure will not collapse. In this way, no additional support structure is needed. The printed structure is given in Fig 18.

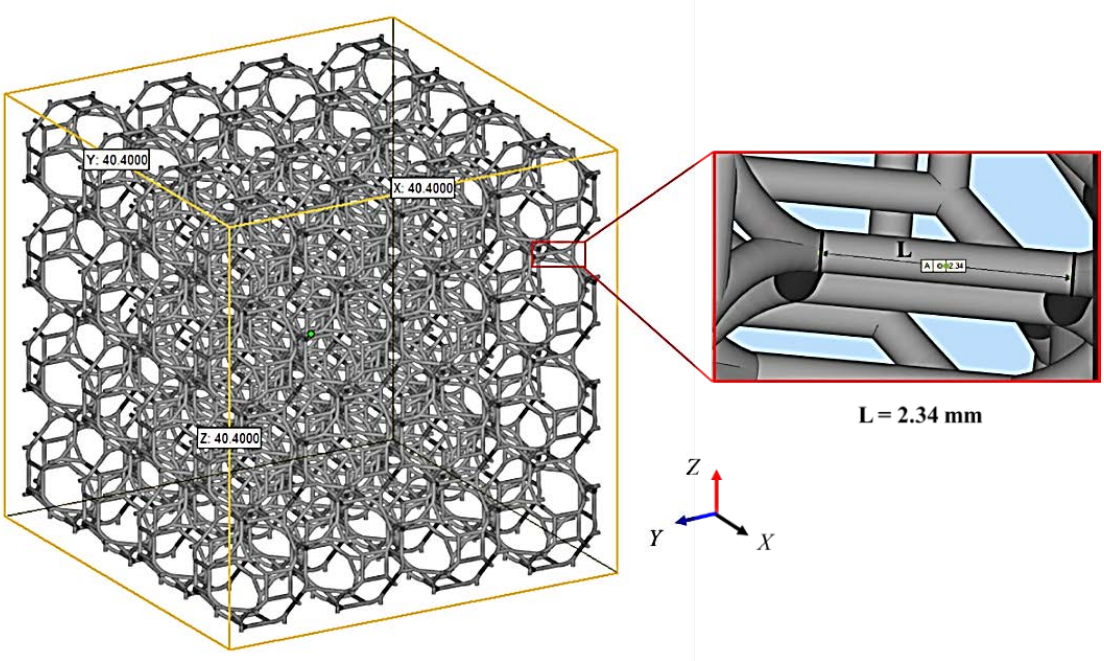

Fig. 17 Structural prototype and cantilever strut analysis in SLM process

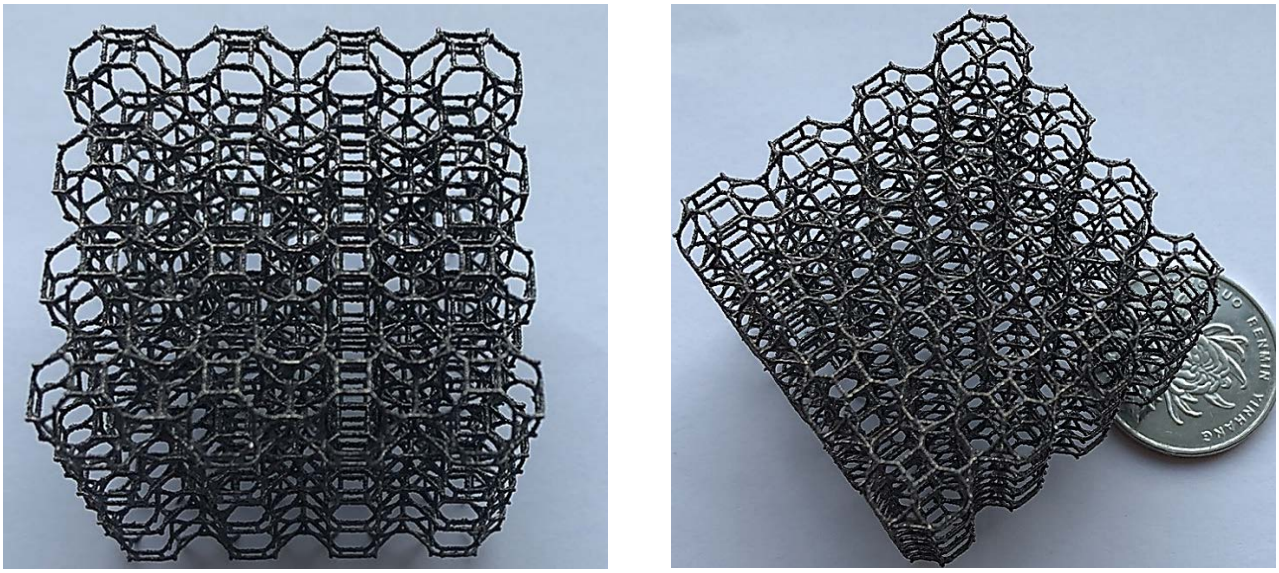

Fig 18. Microstructural arrays using SLM technique (Aluminum alloy: AlSi10Mg)

6. Conclusion

This paper has implemented, for the first time, the design of three-dimensional solid pentamode metamaterials using topological optimization. Then the design problem is formulated to achieve an ultra-lightweight high-performance micro-lattice subject to an ultra-low density and high-resolution in computation. The SIMP-based topology optimization together with the numerical homogenization method is applied to implement the 3D solid pentamode micro-lattices. The topologically optimized designs show the effective properties of the microstructure align with the fundamentals of pentamode materials, including an effective Poisson's ratio close to 0.5, a realistically large (B/G) ratio of the bulk modulus over shear modulus in magnitude, and 5 out of 6 eigenvalues of the elasticity tensor are relatively much smaller in orders. Hence, when the effective Poisson's ratio under appropriate symmetry and isotropy approaches to 0.5, the micro-lattice can mimic the behavior of isotropic pentamode materials. In ANSYS, we first extracted the topological skeleton of the design and established a parameterized model for finite element analysis, and then the subsequent size optimization with ANSYS solver was conducted under different beam diameters, in order to investigate the influence of the geometric sizes on the properties of the pentamode micro-lattices. The results from the size optimization demonstrated that under a given topology the geometric dimensions (e.g. the beam diameter) of the isotropic microstructure have an important impact on its properties. A smaller diameter indicates a better approximation of the effective properties. Finally, the up-to-date additive manufacturing technique (SLM) is used to prototype the optimized specimen. The computational design-manufacturing methodology in this paper can be easily extended to the design of more advanced mechanical micro-lattice metamaterials.

Acknowledgments

This research is supported by Australian Research Council (ARC) - Discovery Projects (DP210101353). We would appreciate Professor Bo Song's group (Huazhong University of Science & Technology) in supporting the additive manufacturing of topologically optimized specimen.

References

[1] J. Guedes, N. Kikuchi, Preprocessing and postprocessing for materials based on the homogenization method with adaptive finite element methods, Computer Methods In Applied Mechanics And Engineering, 83 (1990) 143-198.

[2] O. Sigmund, Tailoring materials with prescribed elastic properties, Mechanics Of Materials, 20 (1995) 351-368.

[3] O. Sigmund, A new class of extremal composites, Journal Of The Mechanics And Physics Of Solids, 48 (2000) 397-428.

[4] D.R. Smith, J.B. Pendry, M.C.K. Wiltshire, Metamaterials and negative refractive index, Science, 305 (2004) 788-792.

[5] Y. Huang, S. Liu, J. Zhao, Optimal design of two-dimensional band-gap materials for uni-directional wave propagation, Structural And Multidisciplinary Optimization, 48 (2013) 487-499.

[6] W. Chen, X. Tian, R. Gao, S. Liu, A low porosity perforated mechanical metamaterial with negative Poisson's ratio and band gaps, Smart Materials and Structures, 27 (2018) 115010.

[7] D. Schurig, J.J. Mock, B.J. Justice, S.A. Cummer, J.B. Pendry, A.F. Starr, D.R. Smith, Metamaterial Electromagnetic Cloak at Microwave Frequencies, Science, 314 (2006) 977.

[8] W. Cai, U.K. Chettiar, A.V. Kildishev, V.M. Shalaev, Optical cloaking with metamaterials, Nature Photonics, 1 (2007) 224-227.

[9] H. Chen, C.T. Chan, Acoustic cloaking in three dimensions using acoustic metamaterials, Applied Physics Letters, 91 (2007) 183518.

[10] A. Sihvola, Metamaterials in electromagnetics, Metamaterials, 1 (2007) 2-11.

[11] D.J. Colquitt, M. Brun, M. Gei, A.B. Movchan, N.V. Movchan, I.S. Jones, Transformation elastodynamics and cloaking for flexural waves, Journal Of The Mechanics And Physics Of Solids, 72 (2014) 131-143.

[12] E. Andreassen, B.S. Lazarov, O. Sigmund, Design of manufacturable 3D extremal elastic microstructure, Mechanics Of Materials, 69 (2014) 1-10.

[13] Y. Wang, Z. Luo, N. Zhang, Z. Kang, Topological shape optimization of microstructural metamaterials using a level set method, Computational Materials Science, 87 (2014) 178-186.

[14] Z. Xiaoyu, L. Howon, T.H. Weisgraber, S. Maxim, D.O. Joshua, E.B. Duoss, J.D. Kuntz, M.M. Biener, G. Qi, J.A. Jackson, Ultralight, ultrastiff mechanical metamaterials, Science, 344 (2014) 1373-1377.

[15] L. Xia, P. Breitkopf, Design of materials using topology optimization and energy-based homogenization approach in Matlab, Structural And Multidisciplinary Optimization, 52 (2015) 1229-1241.

[16] X. Yu, J. Zhou, H. Liang, Z. Jiang, L. Wu, Mechanical metamaterials associated with stiffness, rigidity and compressibility: A brief review, Progress In Materials Science, 94 (2018) 114-173.

[17] W. Chen, X. Huang, Topological design of 3D chiral metamaterials based on couple-stress homogenization, Journal Of The Mechanics And Physics Of Solids, 131 (2019) 372-386.

[18] L. Sam Hyeon, P. Choon Mahn, S.Y. Mun, W.Z. Guo, K. Chul Koo, Composite acoustic medium with simultaneously negative density and modulus, Physical Review Letters, 104 (2010) 054301-054715.

[19] X. Man, Z. Luo, J. Liu, B. Xia, Hilbert fractal acoustic metamaterials with negative mass density and bulk modulus on subwavelength scale, Materials and Design, 180 (2019) 107911.

[20] S. Burns, Negative Poisson's Ratio Materials, Science, 238 (1987) 551-551.

[21] H. Li, Z. Luo, L. Gao, P. Walker, Topology optimization for functionally graded cellular composites with metamaterials by level sets, Computer Methods In Applied Mechanics And Engineering, 328 (2017) 340-364.

[22] R. Lakes, Foam Structures with a Negative Poisson‘s ratio, Science, 235 (1987) 1038.

[23] J.K. Guest, J.H. Prévost, Design of maximum permeability material structures, Computer Methods In Applied Mechanics And Engineering, 196 (2007) 1006-1017.

[24] A.R. Diaz, O. Sigmund, A topology optimization method for design of negative permeability metamaterials, Structural And Multidisciplinary Optimization, 41 (2010) 163-177.

[25] J.S.O. Evans, Negative thermal expansion materials, Journal of the Chemical Society, Dalton Transactions, (1999) 3317-3326.

[26] W. Wu, D. Qi, H. Liao, G. Qian, L. Geng, Y. Niu, J. Liang, Deformation mechanism of innovative 3D chiral metamaterials, Scientific Reports, 8 (2018) 12575.

[27] G.W. Milton, A.V. Cherkaev, Which Elasticity Tensors are Realizable?, Journal of Engineering Materials and Technology, 117 (1995) 483-493.

[28] M. Kadic, T. Bückmann, N. Stenger, M. Thiel, M. Wegener, On the practicability of pentamode mechanical metamaterials, Applied Physics Letters, 100 (2012) 191901.

[29] A. Martin, M. Kadic, R. Schittny, T. Bückmann, M. Wegener, Phonon band structures of three-dimensional pentamode metamaterials, Physical Review B, 86 (2012) 155116.

[30] M. Kadic, T. Bückmann, R. Schittny, M. Wegener, On anisotropic versions of three-dimensional pentamode metamaterials, New Journal Of Physics, 15 (2013) 023029.

[31] T. Bückmann, M. Thiel, M. Kadic, R. Schittny, M. Wegener, An elasto-mechanical unfeelability cloak made of pentamode metamaterials, Nature Communications, 5 (2014) 4130.

[32] M. Kadic, T. Bückmann, R. Schittny, P. Gumbsch, M. Wegener, Pentamode Metamaterials with Independently Tailored Bulk Modulus and Mass Density, Physical Review Applied, 2 (2014) 054007.

[33] Y. Chen, X. Liu, G. Hu, Latticed pentamode acoustic cloak, Scientific Reports, 5 (2015) 15745.

[34] Q. Li, J.S. Vipperman, Three-dimensional pentamode acoustic metamaterials with hexagonal unit cells, The Journal of the Acoustical Society of America, 145 (2019) 1372-1377.

[35] X. Guo, G.-D. Cheng, Recent development in structural design and optimization, Acta Mechanica Sinica, 26 (2010) 807-823.

[36] N.P. van Dijk, K. Maute, M. Langelaar, F. van Keulen, Level-set methods for structural topology optimization: a review, Structural And Multidisciplinary Optimization, 48 (2013) 437-472.

[37] M.P. Bendsøe, N. Kikuchi, Generating optimal topologies in structural design using a homogenization method, Computer Methods In Applied Mechanics And Engineering, 71 (1988) 197-224.

[38] M. Zhou, G.I.N. Rozvany, The COC algorithm, part II: topological, geometry and generalized shape optimization, Computer Methods In Applied Mechanics And Engineering, 89 (1991) 309-336.

[39] O. Sigmund, A 99 line topology optimization code written in Matlab, Structural And Multidisciplinary Optimization, 21 (2001) 120-127.

[40] M.P. Bendsøe, O. Sigmund, Topology Optimization: Theory, Methods, and Applications, Springer, Berlin, 2003.

[41] Y.M. Xie, G.P. Steven, A simple evolutionary procedure for structural optimization, Computers and Structures, 49 (1993) 885-896.

[42] X. Huang, Y.M. Xie, A further review of ESO type methods for topology optimization, Structural And Multidisciplinary Optimization, 41 (2010) 671-683.

[43] J.H. Zhu, W.H. Zhang, K.P. Qiu, Bi-Directional Evolutionary Topology Optimization Using Element Replaceable Method, Computational Mechanics, 40 (2006) 97.

[44] M.Y. Wang, X. Wang, D. Guo, A level set method for structural topology optimization, Computer Methods In Applied Mechanics And Engineering, 192 (2003) 227-246.

[45] G. Allaire, F. Jouve, A.M. Toader, Structural optimization using sensitivity analysis and a level-set method, Journal Of Computational Physics, 194 (2004) 363-393.

[46] Z. Luo, M.Y. Wang, S. Wang, P. Wei, A level set-based parameterization method for structural shape and topology optimization. Int J Numer Methods Eng, International Journal For Numerical Methods In Engineering, 76 (2010) 1-26.

[47] Y. Wang, Z. Luo, Z. Kang, N. Zhang, A multi-material level set-based topology and shape optimization method, Computer

Methods In Applied Mechanics And Engineering, 283 (2015) 1570-1586.
[48] T. Yamada, K. Izui, S. Nishiwaki, A. Takezawa, A topology optimization method based on the level set method incorporating a fictitious interface energy, Computer Methods In Applied Mechanics And Engineering, 199 (2010) 2876-2891.
[49] I. Gibson, D.W. Rosen, B. Stucker, Design for Additive Manufacturing, in: I. Gibson, D.W. Rosen, B. Stucker (Eds.) Additive Manufacturing Technologies: Rapid Prototyping to Direct Digital Manufacturing, Springer US, Boston, MA, 2010, pp. 299-332.
[50] H. Zhang, Z. Kang, Y. Wang, W. Wu, Isotropic "Quasi-Fluid" Metamaterials Designed by Topology Optimization, Advanced Theory and Simulations, 3 (2020) 1900182.
[51] R. Yera, N. Rossi, C.G. Méndez, A.E. Huespe, Topology design of 2D and 3D elastic material microarchitectures with crystal symmetries displaying isotropic properties close to their theoretical limits, Applied Materials Today, 18 (2020) 100456.
[52] N. Rossi, R. Yera, C.G. Méndez, S. Toro, A.E. Huespe, Numerical technique for the 3D microarchitecture design of elastic composites inspired by crystal symmetries, Computer Methods In Applied Mechanics And Engineering, 359 (2020) 112760.
[53] M.P. Bendsøe, O. Sigmund, Material interpolation schemes in topology optimization, Archive Of Applied Mechanics, 69 (1999) 635-654.
[54] O. Sigmund, J. Petersson, Numerical instabilities in topology optimization: A survey on procedures dealing with checkerboards, mesh-dependencies and local minima, Structural optimization, 16 (1998) 68-75.
[55] G.I.N. Rozvany, Aims, scope, methods, history and unified terminology of computer-aided topology optimization in structural mechanics, Structural And Multidisciplinary Optimization, 21 (2001) 90-108.
[56] E. Andreassen, C.S. Andreasen, How to determine composite material properties using numerical homogenization, Computational Materials Science, 83 (2014) 488-495.
[57] J. Gao, H. Xue, L. Gao, Z. Luo, Topology optimization for auxetic metamaterials based on isogeometric analysis, Computer Methods In Applied Mechanics And Engineering, 352 (2019) 211-236.
[58] J. Wu, Z. Luo, H. Li, N. Zhang, Level-set topology optimization for mechanical metamaterials under hybrid uncertainties, Computer Methods In Applied Mechanics And Engineering, 319 (2017) 414-441.
[59] C.M. Zener, S. Siegel, Elasticity and Anelasticity of Metals, The Journal of Physical and Colloid Chemistry, 53 (1949) 1468-1468.
[60] K. Svanberg, The method of moving asymptotes—a new method for structural optimization, International Journal For Numerical Methods In Engineering, 24 (1987) 359-373.
[61] G.D. Cheng, Y.W. Cai, L. Xu, Novel implementation of homogenization method to predict effective properties of periodic materials, Acta Mechanica Sinica, 29 (2013) 550-556.
[62] I. Gibson, D. Rosen, B. Stucker, Additive Manufacturing Technologies, Springer2015.
[63] J. Zhang, B. Song, Q. Wei, D. Bourell, Y. Shi, A review of selective laser melting of aluminum alloys: Processing, microstructure, property and developing trends, Journal of Materials Science and Technology, 35 (2019) 270-284.